https://doi.org/10.5194/egusphere-2025-5728
Preprint. Discussion started: 5 December 2025

Quality Assessment of the AC SAF GOME-2 gridded ozone profile data records

Olaf N.E. Tuinder[1,*], Andy W. Delcloo[2,3*], and Peggy Achtert[4,5,*]

[1]Royal Netherlands Meteorological Institute, Utrechtseweg 297, De Bilt, The Netherlands
[2]Royal Meteorological Institute of Belgium, Observations Department, ACM[2]-team, Ringlaan 3,B-1080 Ukkel, Belgium
[3]Ghent University, Department of Physics and Astronomy, Krijgslaan 281/S9, B-9000, Ghent, Belgium
[4]Deutscher Wetterdienst, Hohenpeissenberg, D-82383, Germany
[5]Leipzig Institute for Meteorology, Leipzig University, Stephanstraße 3, 04103 Leipzig, Germany
[*]These authors contributed equally to this work.

Correspondence: Olaf N.E. Tuinder (olaf.tuinder@knmi.nl)

Abstract. One of the objectives of the Atmospheric Composition SAF is to produce satellite-derived monthly mean data records that are valuable for operational, scientific, and other applications. One of these data records is the gridded global GOME-2A/B/C ozone profile data set presented in this paper. This data record covers the period 2007–2024 and consists of ozone partial columns on a $0.25° \times 0.25°$ grid with 40 vertical layers, with the associated (averaged) averaging kernel (AK) and the a priori needed to use the data in other applications. This paper presents the GOME-2 instrument, the (level-2) ozone profile retrieval method and the subsequent gridding procedure used to generate the level-3 product. We discuss the methodology for averaging AKs in latitude bands and demonstrate that the principal structural features are preserved. We provide a description of the balloon sounding, lidar, FTIR and microwave radiometers validation data and methods, and then perform a quality assessment of the gridded ozone profile product through comparison with these independent data sources for the tropics, mid-latitude and polar latitude bands and in three vertical regions: the Troposphere, and the Lower and Upper Stratosphere. Detailed analyses of absolute and relative differences are provided for each region and height range. The results demonstrate a high level of consistency across the three GOME-2 instruments (with GOME-2A used only up to 2018), underscoring the reliability of the GOME-2 constellation for long-term ozone monitoring. In the troposphere, all three sensors tend to slightly overestimate ozone, with absolute differences (AD) of roughly +1 to +3 DU in mid-latitudes and up to +7.5 DU in the tropics for Metop-C. In lower stratosphere, all sensors show a small negative bias, typically between -3 and -7 DU (RD $\approx$ -3 % to -7 %), corresponding to a modest underestimation of ozone concentrations. In the upper stratosphere, biases are minimal across all sensors, with absolute difference values, close to zero (-0.1 to -0.4 DU) and extremely low variability (STDEV $\approx$ 0.1–0.2 DU). These findings underscore the reliability of the GOME-2 constellation for long-term ozone analyses and the potential for merged multi-sensor time series without significant inter-calibration artifacts suitable for climate and atmospheric research.

https://doi.org/10.5194/egusphere-2025-5728
Preprint. Discussion started: 5 December 2025

1 Introduction

Monitoring atmospheric composition is essential due to several human-induced changes in the atmosphere, such as global warming, stratospheric ozone depletion, increased ultraviolet radiation, and air pollution. In addition, such monitoring enables timely responses to natural hazards and provides the scientific basis for evaluating the effectiveness of international agreements, such as the 1987 Montreal Protocol and its amendments.

The Montreal Protocol, implemented in 1989, has been instrumental in reducing the atmospheric concentrations of ozone-depleting substances. As a result, the ozone layer is on a path to recovery. Recent assessments indicate that total column ozone is expected to return to 1980 levels by around 2040 for the near-global average (60°S–60°N), around 2045 for the Arctic, and around 2066 for the Antarctic (WMO, 2022).

However, recovery is not uniform across all regions and altitudes. While ozone in the upper stratosphere has increased significantly — by approximately 1–3% per decade since 2000 (Steinbrecht et al., 2017) — this increase is most pronounced in the mid-latitudes of both hemispheres (Godin-Beekmann et al., 2022). In contrast, the lower stratosphere, particularly in the tropics and mid-latitudes, has not shown clear signs of recovery (Bognar et al., 2022). The increase in upper stratospheric ozone is primarily driven by two factors: the decline in stratospheric chlorine loading following the implementation of the Montreal Protocol, and cooling of the upper stratosphere, which slows ozone-destroying catalytic cycles and enhances ozone production via ter-molecular reactions (Steinbrecht et al., 2025). This vertical and regional discrepancy highlights the importance of sustained, detailed observations of ozone profiles (WMO, 2018). Satellite-based measurements are central to these global monitoring efforts, providing consistent, long-term, and spatially comprehensive data records of key atmospheric constituents. Ozone remains a particularly critical species in this context, as stratospheric ozone protects life on Earth from harmful ultraviolet radiation from the Sun, while tropospheric ozone acts as a pollutant and greenhouse gas.

This study focuses on the gridded ozone profile products, generated within the framework of the EUMETSAT Atmospheric Composition Satellite Application Facility (AC SAF). These data records are retrieved from measurements of the Global Ozone Monitoring Experiment-2 (GOME-2) instruments onboard the Metop-A, Metop-B, and Metop-C satellites (launched in 2006, 2012 and 2019 respectively). Together, these platforms provide a multi-decadal dataset suitable for long-term assessments.

High-quality ozone profile records are essential for reliable trend detection and are expected to contribute to global assessments such as the World Meteorological Organization (WMO) Scientific Assessment of Ozone Depletion. Therefore, a rigorous validation of the GOME-2 gridded ozone profile data records is required to quantify their accuracy, stability, and suitability for scientific and policy-relevant applications.

In recent years, the time series of satellite-based instruments of the GOME-type (including GOME-2) have been central to construct long-term, harmonised ozone profile and tropospheric ozone datasets. Coldewey-Egbers et al. (2025) present the GOP-ECV record, spanning 1995 to 2021, which merges nadir UV/visible measurements from GOME, SCIAMACHY, OMI and GOME-2 into monthly mean partial columns (19 layers, surface to 80 km) on a $5^\circ \times 5^\circ$ grid by carefully harmonizing inter-sensor differences and aligning with the GTO-ECV total-ozone record. Arosio et al. (2025) provide an inter comparison study between existing tropospheric ozone-column datasets derived from combined nadir- and limb-observations, assessing

https://doi.org/10.5194/egusphere-2025-5728
Preprint. Discussion started: 5 December 2025

consistency, bias and trend detectability. Keppens et al. (2025) further address the harmonization challenge by combining sixteen tropospheric-ozone satellite records (including GOME-2-derived products) to strengthen confidence in tropospheric ozone time-series and their long-term behavior. Regional studies such as Gaudel et al. (2024) exploit satellite records (including IASI/GOME-2) and in situ profiles to quantify tropical tropospheric ozone trends and regional burdens, while Okamoto et al. (2024) apply a multispectral IASI + GOME-2 approach over the tropical Atlantic together with aircraft data to discern natural (biomass burning, stratosphere-troposphere exchange) versus anthropogenic influences on tropospheric ozone variability. Collectively, these works demonstrate that GOME-2 and related sensors now underpin robust ozone-profile and tropospheric-ozone time-series, enabling assessments of spatial distribution, long-term trends and attribution of ozone changes. This paper presents a comprehensive quality assessment of the monthly mean gridded GOME-2A/B/C ozone profile data records. Validation is based on intercomparisons with independent ground-based measurements: ozonesondes, lidar, fourier transform infrared (FTIR) and microwave radiometers (MWR). The focus is on characterizing the performance of the data products in different atmospheric regions (troposphere, lower, and upper stratosphere) and over various latitudinal bands, using monthly averaged profiles to evaluate the long-term consistency and bias structure of the dataset.

2 Ozone profiles from GOME-2

2.1 The GOME-2 instrument

The Global Ozone Monitoring Experiment 2 (GOME-2) are a series of nadir viewing instruments mounted on the Metop satellite series. These instruments fly in a polar orbit around the Earth and have an equator overpass time around 09:30 local solar time. The instrument uses back scattered light from the Sun in the UV-VIS spectral region (240-790 nm). The nominal swath width is 1920 km on the Earths surface with 24 pixels in the forward scanning direction of 80×40 km^2 (cross track $\times$ along track). With the (nominal) wide swath width, global coverage can be achieved in 2 days.

In Table 1 the measurement modes and time periods included in this study are given. The GOME-2A instrument has gone through a number of modes. In December of 2008 the wavelength separation of band-1A / band-1B was shifted from 300 nm to 283 nm, resulting in stratospheric information with smaller footprints. In mid-July 2013, the swath width was changed from the nominal 1920 km to 960 km, which remained until the End of Life de-orbit and shut down of the Metop-A platform in 2021. GOME-2B and GOME-2C have run in the same wide configuration since they were launched.

2.2 Vertical ozone profile retrieval

While the details of the ozone profile retrieval algorithm used to produce the ozone data are given in the ATBD of the Near Real Time (NRT), Offline and Data Record Vertical Ozone Profile and Tropospheric Ozone Column Products (Tuinder et al., 2022), we will provide a description of the relevant aspects of the algorithm below.

https://doi.org/10.5194/egusphere-2025-5728
Preprint. Discussion started: 5 December 2025

The Ozone Profile Retrieval Algorithm (Opera) retrieves vertical ozone profiles from GOME-2 data using the 265 nm–330 nm (UV-VIS) spectral range from the Main Science Channels in band-1a, 1b and 2b. Because of the longer integration time, the band-1a is used across multiple smaller band-1b/2b measurements.

The retrieved information consists of a vertical ozone profile of 40 ozone partial column density values (in DU) on a fixed pressure grid from the surface to 0.001 hPa, a fitted albedo value (either surface albedo or cloud albedo) and an additional offset to correct for a systematic bias in band-1A (possibly a result of stray light or signal leakage). The fixed pressure grid is adjusted to the surface height and, in case of clouds, to the cloud top height.

The LIDORT-A radiative transfer model (Spurr et al., 2008) is used in combination with a polarization correction. For the inversion we use Optimal Estimation, iteratively reaching a converged state of the atmosphere.

Based on the GOME-2 measurement alone, the ozone profile is under-defined, and therefore an a priori ozone profile climatology is used (resolved in latitude bands and months) (McPeters and Labow , 2012).

The (initial) surface albedo comes from the GOME-2 version 3 surface DLER database (see Tilstra et al. (2017, 2021)). The initial cloud albedo is set to 0.8.

Spectral spikes, such as those caused by highly energetic particles common over the South Atlantic Anomaly region, are removed by starting at 290 nm and filtering out all peaks below that wavelength above 4σ (where σ is the reflectance error), relative to the higher (valid) reflectance measurement. If there are more than 30 peaks removed, the remaining spectrum below the last valid is removed completely because the reference measurement is no longer representative.

2.2.1 Degradation correction

The GOME-2 instrument degrades over time, i.e. the signal level measured by the detector decreases with time, either through effects in the optical light path (including the scan mirror) or the sensitivity of the photon detector itself is affected (or both) (EUMETSAT, 2022). One complicating factor is that the measured radiance from the Earth degrades in a different way than the irradiance measured from the Sun, so they do not fully cancel out when the reflectance is calculated. In order to compensate for the long term instrument degradation, correction polynomials are fitted based on the ratio of daily averaged measured and calculated reflectance. The latter were generated by providing the forward model with an ozone profile from the climatology scaled with expected ozone columns from an assimilated ozone field.

Instrument	Swath	Period	Remarks
GOME-2A	Wide	2007-01-01 – 2008-12-10	original 1a/1b setting
"	Wide	2008-12-10 – 2013-07-15	1a/1b shift wide swath
"	Small	2013-07-15 – 2021-11-15	small swath until End Of Life
GOME-2B	Wide	2013-01-01 – 2024-12-31	currently flying
GOME-2C	Wide	2019-01-01 – 2024-12-31	currently flying

Table 1. Measurement modes for GOME-2A/B/C

https://doi.org/10.5194/egusphere-2025-5728
Preprint. Discussion started: 5 December 2025

2.3 Averaging Kernels

An averaging kernel (AK) matrix of an optimal estimation inversion is a linear representation of the weights of the effect of a change in the fitted parameters on the retrieved value at a specific position in the state vector (Rodgers et al., 1990). In other words, it represents how changes in the ozone partial column at various layers along the vertical model atmosphere affect the outcome of a particular retrieved layer. In an optimal retrieval, the AK would be close to the identity matrix, but in real world situations vertical resolution of a retrieved profile is wider, and can span multiple layers or even the whole atmosphere.

The retrieved ozone profile depends on the a priori, the true ozone profile and the averaging kernel according to the following relationship (Equation 1):

$$X_{retrieved} = X_{a\ priori} + AK(X_{true} - X_{a\ priori}) \tag{1}$$

where X denotes a state vector (i.e.: the list of values: the ozone profile, albedo and offset), and the subscripts indicate the type of vector. Unfortunately, the averaging kernel can not be inverted (due to singularity), so the X_{true} cannot be calculated on its own; it is always dependent on the other components and the relationship described above. Therefore a reference data set with a high vertical resolution can be easily compared to a satellite data set, not the other way around. In section 3.3 we will revisit the topic of averaging kernels.

3 The gridding from level-2 to level-3

3.1 The gridding method

The gridded level-3 ozone profile product is created based on a grid definition, which sets the name of the variable, the name of the source parameter, and the number of latitudes, longitudes and vertical layers in which to divide the horizontal and the vertical dimension. The default horizontal resolution is $0.25° \times 0.25°$ with 40 vertical layers from the surface to 0.001 hPa.

The ground footprint of each retrieved vertical ozone profile is divided into equal footprint-sub-cells (4 along track $\times$ 8 across track) which are projected (binned) onto the fixed grid. At the end of the data binning, the averaged value, the standard deviation and other variables are calculated.

3.2 Calculated parameters

In the gridded ozone profile product, we provide the arithmetic mean, the population standard deviation associated with the arithmetic mean, the weighted mean (weighted by the error values of the parameter, if available) and the standard error of the weighted mean.

The arithmetic mean value in a grid cell is calculated as follows:

$$\text{Arithmetic Mean} = \frac{\sum_{\mathrm{n=1}}^{\mathrm{N}} \mathrm{x_i}}{\mathrm{N}} \tag{2}$$

where x_i is the individual data point and N is the number of data points. In order to calculate the arithmetic mean, the number of data points in a grid cell and the sum of the data values in that grid cell are stored. This enables daily grids to be merged into

https://doi.org/10.5194/egusphere-2025-5728
Preprint. Discussion started: 5 December 2025

monthly grids and monthly grids into yearly grids, without loss of information. This also applies to re-gridding onto coarser horizontal resolutions which can also be calculated without loss of information.

The population standard deviation σ in a grid cell is calculated as follows:

$$\sigma = \sqrt{\frac{\sum (x - \bar{x})^2}{N}} \tag{3}$$

$$\sigma = \sqrt{\left(\frac{1}{N}\sum_{n=1}^{N} x_i^2\right) - \left(\frac{1}{N}\sum_{n=1}^{N} x_i\right)^2} \tag{4}$$

$$\sigma = \frac{\sqrt{N\left(\sum_{n=1}^{N} x_i^2\right) - \left(\sum_{n=1}^{N} x_i\right)^2}}{N} \tag{5}$$

In order to calculate the standard deviation, the sum of the squared data values ($\sum_{n=1}^{N} x_i^2$) needs to be stored, in addition to the sum of the values (already stored).

If the weight of the weighted mean is taken as 1/variance = 1/($error_i^2$), then the weighted mean and the standard error can be written as:

$$\text{Weighted Mean} = \frac{\sum_{\mathrm{n=1}}^{\mathrm{N}} \left(\mathrm{x_i}/(\mathrm{error_i})^2\right)}{\sum_{\mathrm{n=1}}^{\mathrm{N}} \left(1/(\mathrm{error_i})^2\right)} \tag{6}$$

$$\text{Standard Error} = \frac{1}{\sum_{\mathrm{n=1}}^{\mathrm{N}} \left(1/(\mathrm{error_i})^2\right)} \tag{7}$$

If one keeps track of two sums:

$$\mathrm{SumValDivSqErr} = \sum_{\mathrm{n=1}}^{\mathrm{N}} \left(\mathrm{x_i}/(\mathrm{error_i})^2\right) \tag{8}$$

$$\mathrm{SumOneDivSqErr} = \sum_{\mathrm{n=1}}^{\mathrm{N}} \left(1/(\mathrm{error_i})^2\right) \tag{9}$$

then the weighted mean and the standard error can be written as:

$$\text{Weighted Mean} = \frac{\mathrm{SumValDivSqErr}}{\mathrm{SumOneDivSqErr}} \tag{10}$$

$$\text{Standard Error} = \sqrt{\frac{1}{\mathrm{SumOneDivSqErr}}} \tag{11}$$

For parameters where there is no error available a unity value is taken (i.e.: 1.0).

Table 2 lists the primary and derived values that are stored in the gridded ozone profile product.

https://doi.org/10.5194/egusphere-2025-5728
Preprint. Discussion started: 5 December 2025

Primary values	Derived values
the number of sub-pixels seen	the arithmetic mean (Eq. 2)
the minimum value of all data point values	the arithmetic mean (Eq. 2)
the maximum value of all data point values	the standard deviation (Eq. 3)
the sum of the data point values	the weighted mean (Eq. 10)
the sum of the square of each of the data point values	the weighted mean error (Eq. 11)
SumValDivSqError (Eq. 8)	
SumOneDivSqError (Eq. 9)	

Table 2. Primary and derived values stored in the gridded GOME-2 ozone profile product

3.3 Gridded averaging kernel

As explained earlier in section 2.3, the AK of the ozone profile describes the linear effect (weights) of ozone in all atmospheric layers on a particular (nominal) retrieved layer. In the level-2 ozone data, each individual retrieved profile has 40 layers and the associated AK matrix has 40×40 elements. While it is technically possible to store gridded / averaged AKs for all $0.25° \times 0.25°$ grid cells, this would make a regular level-3 gridded data product 40 times larger and unwieldy to use. As an alternative we have chosen to grid / average all AKs in 18 bands of $10°$ latitude.

An example of such a gridded / averaged AK is shown in Figure 1, where for March 2019 the GOME-2B AK matrix for the latitude band at $45°$ N is shown on the left, and the weight curves for the nominal layers are shown in the middle. In the matrix plot, the x-axis (x_i) can be seen as the nominal retrieved layer index, and the y-axis then represents the index of the weights of the contributing layers to the particular nominal layer at index x_i. Also shown in Figure 1 on the right is the ozone profile and a priori profile at $45°N/0°E$ for the same month, which gives a perspective in the shape of the profile and the position of the ozone maximum in the gridded data.

What stands out is that the bottom four layers have very little sensitivity (the matrix values are green across the vertical). In other words: the GOME-2 retrieved ozone profile is not very sensitive in the troposphere where (on average) relatively little ozone is present. For the next few layers, there is a positive sensitivity close to the nominal (indexed) layer, and a negative or positive weight higher up. Above layer 15, the positive values start a little above the diagonal, which means that the profile is more sensitive to ozone above the nominal layer. For the top eight layers there is also little sensitivity, which corresponds with the upper stratosphere with diminishing ozone as one goes up.

In order to assess the the impact of these positive and negative effects indicated in the AK, we should also take into account the ozone content at those layers location. Even though the weights of the AK curves are fanning out at the top layers, their impact on the retrieved value is relatively small because there is very little ozone above layer 30.

As mentioned above, we longitudinally average the AKs into matrices representative for bands of $10°$ latitude in order to save space in the output product. While this is unconventional, a study done by Johnson et al. (2018) shows that using a representative AK results in relatively small differences in a wide range of ozone profile cases. To explore this a little further,

https://doi.org/10.5194/egusphere-2025-5728
Preprint. Discussion started: 5 December 2025

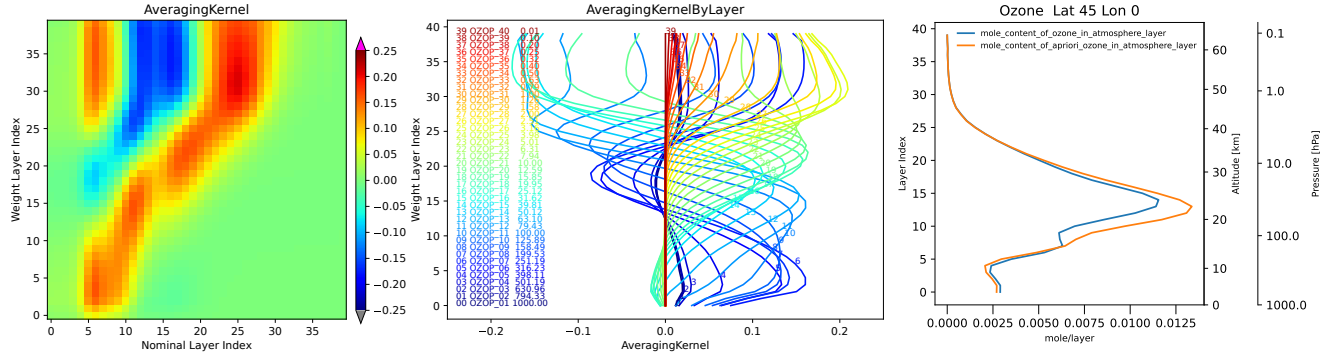

Figure 1. Example of the gridded averaging kernel, for GOME-2B at $45^\circ N$ on March 2019. Left: the averaging kernel matrix; Middle: the weights curves of the layers; Right: the ozone profile and a priori at $45^\circ N/0^\circ E$ in mole for the layer.

we present the variability of the averaging kernels of the co-located level-2 profiles in Uccle in Figure 2. This figure shows the mean of the colocated averaging kernels (top) and the 10th, 50th and 90th percentiles (bottom row) of a full year of level-2 GOME-2A ozone profile retrievals near Uccle (Belgium). The percentile plots provide an indication of the spread of the AK values in the level-2 data used as a source for the level-3. While the change in the AK value along the percentiles is most prominent in the upper stratosphere (above layer 25), this is also the region with diminishing ozone and therefore has a smaller effect on the retrieved ozone. At the same time, the main structure along the diagonal remains intact across the whole range of percentiles in the altitude region where most of the ozone is present. The mean and median (i.e. the 50th percentile) of the averaging kernels are very similar, so in the L3 gridded product we provide the mean because of ease of calculation.

3.4 Time series of parameters

Figure 3 shows a time series of the global arithmetic mean of some of the parameters in the L3 data set, which give a general impression of its behaviour over the mission period. It shows the atmosphere mole content of ozone (i.e.: the full atmosphere), the atmosphere mole content of the lower troposphere (surface to 500 hPa), the number of spectral detector pixels used in the (level-2) retrieval and the degrees of freedom of the resulting profile. Due to specific validity of the spectral ranges of each of the GOME-2 instruments, the number of spectral pixels (NMeasurements) is also different. The degradation of the GOME-2 instrument contributes to a reduction of valid spectral information going into the level-2 retrieval over time. In the case of GOME-2A, the degradation (and quality control of the spectrum) causes an increasingly steep drop off of the number of valid spectral information of GOME-2A after 2018. The effect of this can be seen in an increasing deviation of the total ozone column compared to the other instruments, and especially in the troposphere. The degradation in general also has an effect on the degrees of freedom of the retrieval.

Even though the retrieved level-2 and gridded level-3 data is available to users, we recommend to not use the ozone data from GOME-2A after 2018 and restrict our validation of this instrument therefore up to the end of that year.

https://doi.org/10.5194/egusphere-2025-5728
Preprint. Discussion started: 5 December 2025

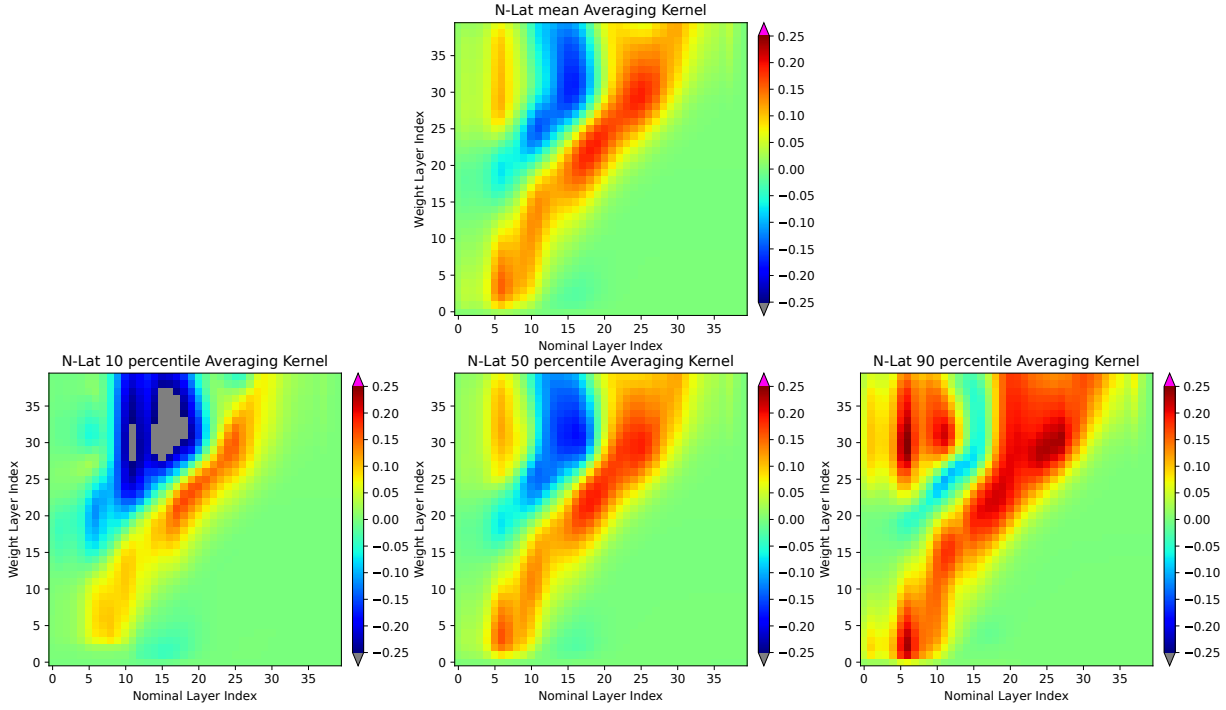

Figure 2. Averaged averaging kernels of GOME-2A ozone profile retrievals near Uccle (Belgium) in 2009: the mean (top), and the 10th, 50th and 90th percentile (bottom row)

4 Validation Data and Methods

The quality assessment of the AC SAF GOME-2A/B/C gridded ozone profile products was carried out using independent ground-based observations. For the lower stratosphere and troposphere, comparisons were made with ozonesonde measurements. Ozonesondes are balloon-borne instruments capable of measuring vertical ozone profiles from the surface up to approximately 30 km, with a much higher vertical resolution (~ 180m) than satellite sensors (WMO, 2018) . In addition, ozonesondes generally provide better precision and accuracy in the lower stratosphere and troposphere. They can also be launched under nearly all meteorological conditions and at any time of day. The precision of ozonesonde measurements varies with altitude and depends on the type of instrument (Stauffer et al., 2022). For this validation study, only the ozonesonde station of Hohenpeissenberg still uses Brewer-Mast ozonesondes. For the Japanese stations we can report that KC sondes were operational until December 2009. The other stations used (Figure 4) in this validation study are all using ECC ozonesondes. Intercomparison campaigns and quality assurance studies have demonstrated systematic differences in precision between electrochemical concentration cell (ECC) and Brewer–Mast (BM) ozonesondes across the troposphere and stratosphere. In the troposphere (surface to $\sim$10 km; $\sim$1000–300 hPa), ECC sondes exhibit high precision, typically within $\pm$3–4% Stubi et al. (2008); Smit et al., (2007); WMO (2014). In the lower to mid-stratosphere (10–30 km; $\sim$300–10 hPa), ECC sondes maintain excellent precision of approximately $\pm$3% across different manufacturers and cathode sensing solutions, while BM sondes show mod-

https://doi.org/10.5194/egusphere-2025-5728
Preprint. Discussion started: 5 December 2025

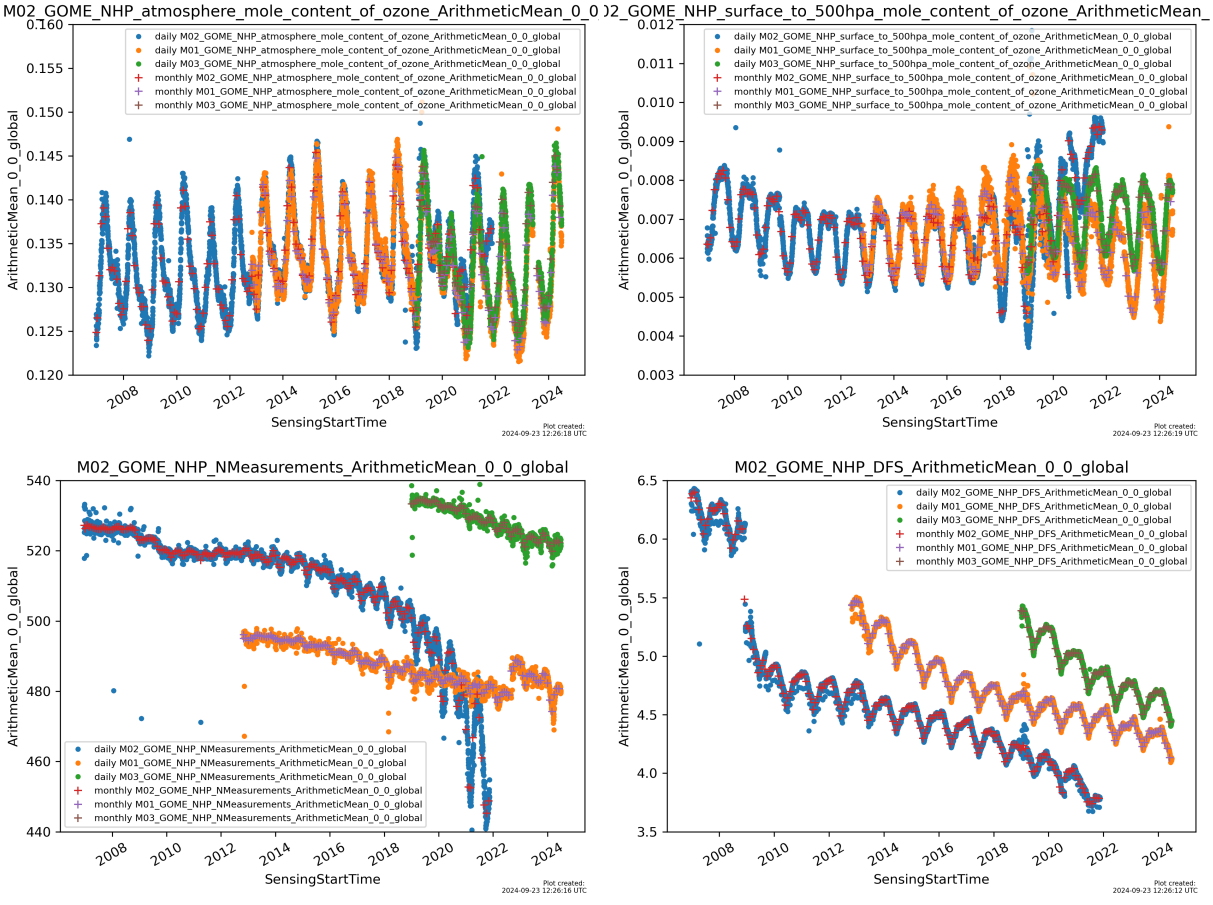

Figure 3. Time series of the global arithmetic mean of some parameters from GOME-2A/B/C jointly for the full available data length in the data record. Both the daily global mean is shown as well as the monthly mean. Top left: mole content of ozone (full vertical column), top right: mole content of ozone from the surface to 500hPa, bottom left: number of spectral detector pixels used in the retrieval, bottom right: number of degrees of freedom in the retrieval.

https://doi.org/10.5194/egusphere-2025-5728
Preprint. Discussion started: 5 December 2025

erate precision of ±3–5% Stubi et al. (2008); WMO (2014). In the upper stratosphere (30–35 km; ∼10–1 hPa), ECC sondes continue to perform well, with uncertainties slightly increasing to ∼3–4%, with best performance reported around 40 hPa near the ozone maximum (Smit et al.,, 2007; WMO, 2014). Recent intercomparison work (Smit et al., 2024) indicates that for ECC ozonesondes the relative uncertainty remains in the order of 5–10 % throughout much of the profile, but rises at pressures below ∼13 hPa (∼30–32 km altitude). For the upper stratosphere (15–60 km), measurements from lidar, FTIR and MWR were used. These instruments extend vertical coverage beyond the range of ozonesondes and provide valuable overlap between 15 km and 30 km. However, global coverage remains limited: only a few long-term lidar (approx. < 5) and MWR (approx. < 4) stations provide regular observations, often with significant delays in data availability. No long-term upper stratospheric observations are available from the southern polar regions.

Lidar systems, typically operating with the Differential Absorption Lidar (DIAL) technique (Godin et al., 1998), provide accurate ozone profiles in clear sky, nighttime conditions of up to about 50 km (Leblanc and McDermid, 2000; Steinbrecht et al., 2006). Usually, 5 to 8 profiles are acquired per month, each requiring several hours of integration depending on the system and the atmospheric conditions. The natural output format of lidar profiles is ozone number density versus geometric altitude.

MWRs retrieve ozone profiles by measuring the pressure-broadened shape of a thermal emission line (Lobsiger et al., 1984; Parrish et al., 1988). Using an optimal estimation technique (Rodgers et al., 1990), these instruments deliver ozone number density profiles typically between 20 km and 60 km altitude. In contrast to lidar, MWRs operate during the day and are less affected by weather conditions. On average, 20 profiles are acquired per month, with integration times between 30 minutes and 5 hours, depending on the instrument (Boyd et al., 2007; Hocke et al., 2007).

Table 3. Typical precision and vertical resolution of lidar and MWR systems (see Steinbrecht et al. (2006)).

Altitude	**Lidar**		**MWR**	
(km)	Precision (%)	Resolution (km)	Precision (%)	Resolution (km)
15	5	1.4		
20	5	1.2	3	10
25	3	1.0	3	10
30	3	1.8	3	10
35	3	4.2	3	14
40	5	7.2	3	14
45	15	8.6	3	20
50	55	8.6	3	20

An FTIR spectrometer measures ozone profiles between 3 and 42 km by analyzing the interaction of infrared radiation with the atmosphere. The instrument records high-resolution infrared spectra. Ozone absorbs certain wavelengths of infrared light due to its molecular structure. The FTIR spectrometer detects this absorption and converts the information into an ozone spectrum using the Fourier transform method. This conversion allows ozone concentrations to be represented as a function of altitude. The total error range is from 1.5 to 2.5% between 250 and 3000 DU (Garcia et al. (2022)) without a simultaneous temperature fit, but around 1.5% when a temperature retrieval is included in the data retrieval.

https://doi.org/10.5194/egusphere-2025-5728
Preprint. Discussion started: 5 December 2025

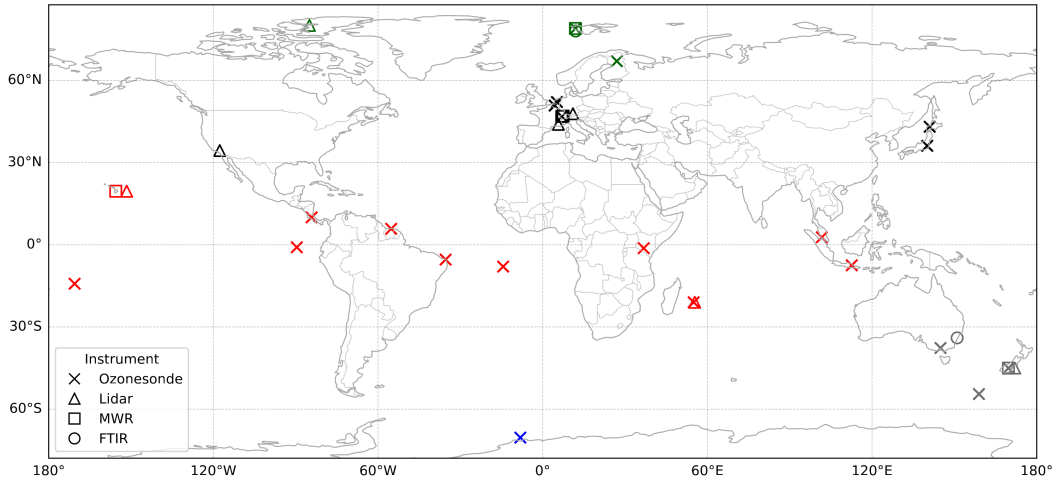

Figure 4. Overview of the stations used for tropospheric and stratospheric quality assessment. Ozonesonde stations are indicated by crosses, lidar stations by triangles, FTIR by circles, and MWR stations by squares. The latitudinal classification is: northern polar stations (green, $67°N - 90°N$), northern mid-latitude stations (black, $30°N - 67°N$), tropical stations (red, $30°N - 30°S$), southern mid-latitude stations (grey, $30°S - 70°S$), and southern polar stations (blue, $70°S - 90°S$).

4.1 Ground-based Dataset Description

Ground-based ozonesonde observations used in this study are available from the World Ozone and Ultraviolet Data Center (WOUDC, http://www.woudc.org) and the NILU Atmospheric Database for Interactive Retrieval (NADIR) hosted by the Norwegian Institute for Air Research (NILU, http://www.nilu.no/nadir/). Ground-based lidar and MWR ozone profiles were obtained from the Network for the Detection of Atmospheric Composition Change (NDACC, http://www.ndsc.ncep.noaa.gov/). All NDACC lidar, FTIR, and MWR instruments undergo a standardized evaluation process and extensive quality control (Keckhut et al., 2004).

Figure 4 provides an overview of the stations used for this validation. Ozonesonde stations are indicated by crosses, lidar stations by triangles, FTIR stations by circles, and MWR stations by squares. The latitudinal classification is as follows: northern polar stations (green, $67°N - 90°N$), northern mid-latitude stations (black, $30°N - 67°N$), tropical stations (red, $30°N - 30°S$), southern mid-latitude stations (gray, $30°S - 70°S$) and southern polar stations (blue, $70°S - 90°S$). For each station, we computed a monthly mean ozone profile and compared it to the monthly mean level-3 ozone data, obtained with a horizontal distance smaller that 100 km around the location of the ground-based stations.

4.2 Pre-processing of ground-based ozone profile Data and Application of Satellite Averaging Kernels

The ground-based ozone lidar, FTIR, and MWR profiles were pre-processed and harmonized with the satellite retrieval grid in order to enable a consistent comparison. The lidar data files contain monthly mean ozone number densities (cm^{-3}) between

https://doi.org/10.5194/egusphere-2025-5728
Preprint. Discussion started: 5 December 2025

approximately 15 and 50 km. The lidar profiles were converted into partial ozone columns expressed in Dobson Units (DU) per layer according to:

$$\mathrm{DU}_{\mathrm{layer}} = \frac{n(z)\,\Delta z_{\mathrm{cm}}}{2.687 \times 10^{16}}, \tag{12}$$

where $n(z)$ is the ozone number density (in cm^{-3}) and Δz_{cm} is the layer thickness in centimeters.

For each month, the corresponding satellite data (retrieved ozone, a priori ozone, averaging kernel, and standard deviation) were extracted from the level-3 NetCDF ozone profile data record files. The satellite quantities, given as ozone column amounts in $\mathrm{mol\,m}^{-2}$, were converted into Dobson Units by using $1\,\mathrm{DU} = 4.462 \times 10^{-4}\,\mathrm{mol\,m}^{-2}$. Ozonesonde data, already available in DU, were integrated over the GOME-2 pressure layers. The vertical coordinates of the satellite layers, originally defined in pressure, were converted to geometric altitude using the U.S. Standard Atmosphere (1976).

The averaging kernels (AKs) provided with the satellite product were applied to the ground-based profiles following (Equation 1) in the Dobson Unit space. All ozone profiles (satellite retrieved, a priori, ground-based, and AK-retrieved ground-based) were subsequently interpolated and re-binned onto a uniform 1-km vertical grid up to 60 km altitude. The re-binning of partial columns from the irregular satellite layers to the uniform grid conserved the total amount of ozone in DU by weighting each layer according to the geometric overlap between the native and target bins. The described processing ensures that the ground-based profiles are expressed on the same vertical grid and smoothing characteristics as the satellite retrievals, thus allowing a direct and consistent validation of the satellite ozone profiles.

For the validation the satellite data as well as the ground-based data were integrated over several altitude bands (e.g. 0–8 km, 14-30 km, 30–40 km, and 40–50 km for mid-latitude levels). These band-integrated ozone columns were used to obtain time series for the ground-based, satellite, and AK-retrieved ground-based datasets.

5 Validation of the GOME-2 Metop-A/B/C level-3 Ozone Profile Dataset

This section describes the validation of the reprocessed GOME-2A/B/C level-3 (gridded) ozone profile products. The validation periods are as follows: January 2007 to December 2018 for GOME-2A, December 2012 to December 2024 for GOME-2B, and January 2019 to December 2024 for GOME-2C.

The validation is structured around the troposphere, lower stratosphere (up to 30 km altitude), and the upper stratosphere. Table 4 defines the vertical ranges used for the troposphere and the lower and upper stratosphere in different latitude bands:

Table 4. Definition of the vertical ranges for the lower and upper stratosphere in different latitude belts.

Region	Troposphere	Lower Stratosphere	Upper Stratosphere
Polar Region	0-6 km	12–30 km	30–50 km
Mid-Latitudes	0-8 km	14–30 km	30–50 km
Tropical Region	0-12 km	18–30 km	30–50 km

https://doi.org/10.5194/egusphere-2025-5728
Preprint. Discussion started: 5 December 2025

For the tropsophere and lower stratosphere, comparisons are made against ozonesonde measurements. For the upper stratosphere, lidar, and microwave radiometer (MWR) data are used as reference. Relative differences are calculated using:

$$\mathrm{RD} = \frac{\text{GOME-2 L3} - \text{retrieved ground-based}}{\text{retrieved ground-based}} \times 100 \tag{13}$$

Table 5. GOME-2A/B/C gridded validation statistics (Absolute Difference [AD], Relative Difference [RD], and standard deviation [STDEV]) for the troposphere, lower and upper stratosphere across latitude regions: Units: AD in DU, RD and STDEV in %.

	Troposphere			Lower Stratosphere			Upper Stratosphere		
Region	AD	RD	STDEV	AD	RD	STDEV	AD	RD	STDEV
Metop A									
Northern Polar	1.3	9.7	8.0	-6.1	-3.9	3.7	-0.2	-7.8	0.2
Northern Mid-Lat.	2.3	14.9	12.3	-6.7	-4.5	4.0	-0.1	-2.8	0.2
Tropics	3.6	27.3	25.5	-3.6	-3.5	3.1	-0.3	-3.9	0.1
Southern Mid-Lat.	0.7	6.7	13.9	-1.6	-1.1	3.3	-0.1	-1.1	0.1
Southern Polar	-0.6	-7.4	11.1	0.5	0.4	4.1	–	–	–
Metop B									
Northern Polar	1.2	8.6	9.5	-4.5	-3.0	4.9	-0.3	-10.5	0.2
Northern Mid-Lat.	2.3	14.7	10.7	-5.9	-3.9	3.2	-0.1	-3.6	0.2
Tropics	2.8	21.9	18.7	-2.7	-2.6	2.2	-0.1	-3.5	0.1
Southern Mid-Lat.	0.5	5.3	10.0	-0.1	-0.2	2.3	-0.1	-1.6	0.1
Southern Polar	-0.8	-9.5	8.2	1.1	0.9	3.8	–	–	–
Metop C									
Northern Polar	0.5	3.5	9.0	-3.3	-2.5	6.1	-0.4	-13.5	0.2
Northern Mid-Lat.	2.4	15.0	10.4	-6.8	-4.7	2.9	-0.2	-4.2	0.2
Tropics	7.5	57.6	28.0	-7.0	-6.8	2.4	-0.2	-4.2	0.1
Southern Mid-Lat.	1.1	11.8	15.7	-2.1	1.7	2.8	-0.1	-1.1	0.2
Southern Polar	-0.6	-7.5	8.8	-0.1	0.1	3.1	-	–	–

Table 5 summarizes the differences between L3 gridded ozone profiles and the ground-based reference data. The relative difference is generally below 15% in the troposphere, except in the tropical troposphere, and both the lower and upper stratosphere for all latitude bands. For the southern polar stations, there was no information available for the upper stratospheric part.

5.1 Validation results for the troposphere and lower stroposphere

To assess the consistency of the GOME-2A/B/C level-3 ozone profile product in the troposphere and lower stratosphere, we compare the integrated ozone values for the tropospheric and lower stratospheric part of GOME-2A/B/C profiles with the

https://doi.org/10.5194/egusphere-2025-5728
Preprint. Discussion started: 5 December 2025

corresponding levels derived from ozonesonde data, following (Table 4). The averaging kernels are applied and those values are used in the evaluation. Figure 5 shows the outcome for the mid-latitude stations and Table 5 summarizes the results for the time periods under consideration for the different latitude belts. The comparison with balloon sondes shows that all three sensors have comparable results and are all within 10 % for the lower stratosphere. We can observe a seasonal dependency, present in the dataset; this was also the case in the level 2 product. Delcloo et al. (2024) did also describe this seasonal dependency for both, the lower stratosphere and troposphere. For the troposphere, we see among all sensors the same behavior, an overestimation of the tropospheric ozone part in the Tropical belt (Delcloo, 2024). Here we note that in this specific region, the retrieved ozone concentrations shows very high differences for the GOME-2C sensor, also in the lower troposphere (see Table 5), for which we have no explanation yet.

For the first two years of the GOME-2A mission, there was a particular instrumental integration time setting for the spectral bands 1A and 1B in the far- and near-UV regions, that made it difficult to distinguish the troposphere from the stratosphere on small ground pixels. This was changed by the end of 2008 (also listed in Table 1). This inconvenient instrument setting has affected the ozone profile across the full atmosphere for the first two years, but this effect should not cause the sustained bias for the first four years of the mission, as seen in Figure 5. Our hypothesis is that the degradation correction, which spans multiple years in order to get the seasonal effect right, has a lingering effect.

5.2 Validation results for the upper stratosphere

To assess the consistency of the GOME-2 monthly mean level-3 ozone profile product in the upper stratosphere, monthly averaged satellite partial columns were compared with ground-based observations. The analysis focuses on the 30–50 km altitude range, where the application of the averaging kernel is essential due to the limited vertical sensitivity of nadir-viewing instruments. The results of the comparison for mid-latitude and tropical stations are presented in Figure 6 and Figure 7, respectively. The mean retrieved ground-based profiles (left panel) closely follow the satellite retrievals, particularly between 40 and 50 km.

The time series of monthly mean ozone partial columns between 30–40 km and 40–50 km (middle panels) show good agreement in both long-term variability and seasonal cycles, with maxima in summer and minima in winter. Although a bias in absolute values is apparent between the satellite and ground-based datasets, the satellite product reliably reproduces the temporal evolution of ozone in the upper stratosphere. The higher correlation between the retrieved ground-based and level-3 time series, compared to that between the original ground-based and level-3 data, highlights the effectiveness of the a priori and averaging kernel corrections and confirms the vertical representativeness of the satellite product. The correlation coefficients for each altitude range are indicated in the middle panels.

The relative bias (left panels in Figure 6 and Figure 7) between the three satellite sensors and the adjusted lidar data (right panels) remains within $\pm 10\%$ in the 30–40 km altitude range. In the 40–50 km region, the relative differences are larger, around 20%, particularly during periods of ozone maxima and minima. Nevertheless, the mean relative difference, as reported in Table 5, is below 5%. Overall, the lidar-based validation confirms the robustness of the GOME-2 level-3 ozone profile product and its suitability for cross-validation with other satellite datasets and the construction of long-term ozone time series.

https://doi.org/10.5194/egusphere-2025-5728
Preprint. Discussion started: 5 December 2025

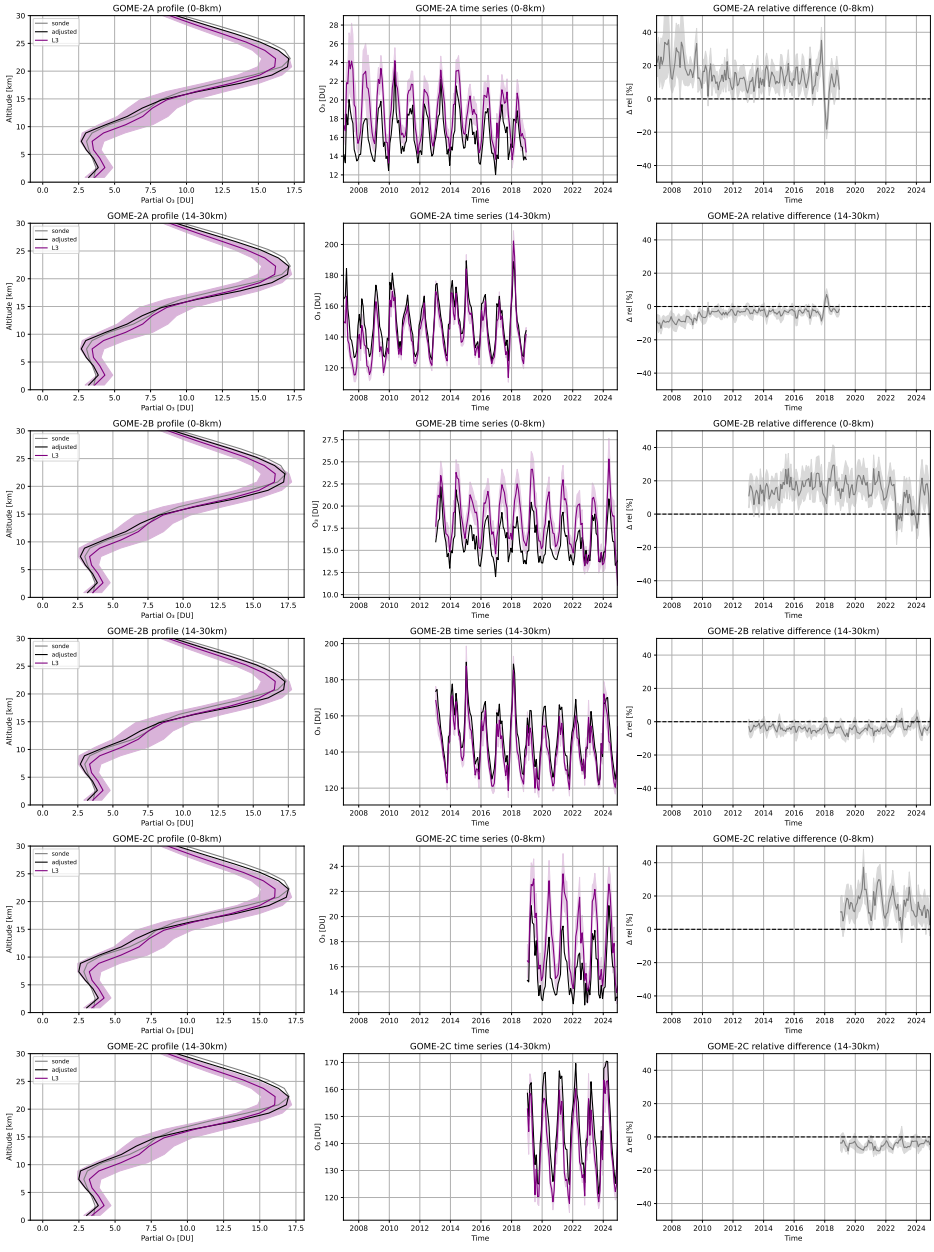

Figure 5. Comparison of ozone partial columns derived from satellite and ground-based observations for GOME-2A/B/C. For each sensor (from top to bottom), the three panels show: (left) the mean vertical profile of ozone partial columns in Dobson Units (DU) averaged over the entire observation period, including the L3 satellite retrieval (purple), the ozonesonde measurement (grey), the ozonesonde profile adjusted by the satellite averaging kernel and a priori profile (black), the L3 a priori profile (green), and the $\pm 1\sigma$ uncertainty of the satellite profile (shaded); (middle) the time series of monthly mean ozone partial columns in the 0–8 km altitude range (troposphere) and in the 14–30 km altitude range (lower stratosphere) for the same data sources; and (right) the relative difference between the L3 and adjusted ozonesonde data in this altitude range. This comprehensive comparison illustrates the consistency between satellite and ground-based ozone observations, as well as systematic differences over time and altitude.

https://doi.org/10.5194/egusphere-2025-5728
Preprint. Discussion started: 5 December 2025

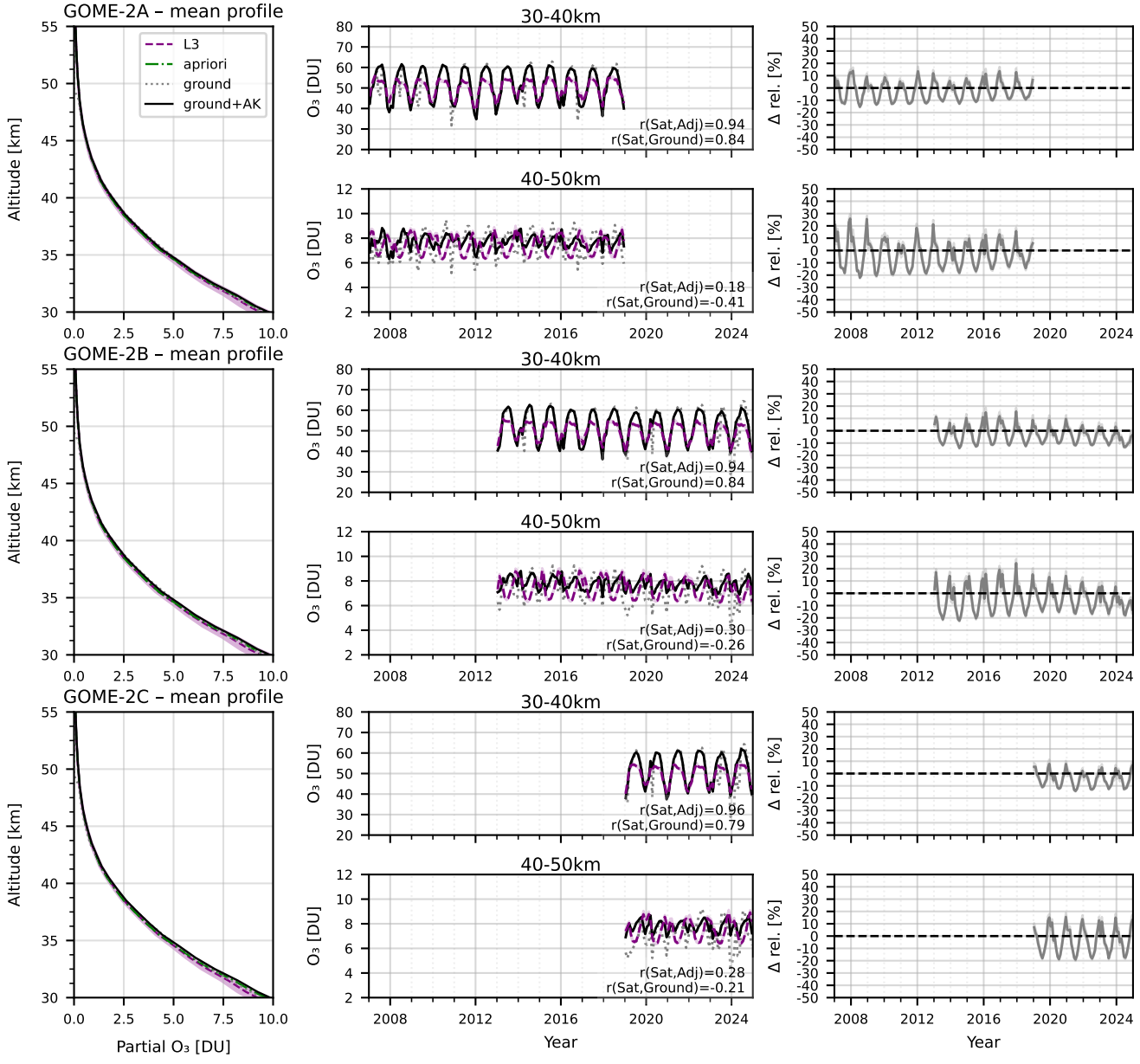

Figure 6. Comparison of ozone partial columns derived from satellite and all mit-latitude ground-based observations as shown in Figure 4, for GOME-2A/B/C. For each sensor (from top to bottom), the three panels show: (left) the mean vertical profile of ozone partial columns in Dobson Units (DU) averaged over the entire observation period, including the L3 satellite retrieval (purple), the lidar measurement (grey), the retrieved lidar profile (black), the L3 a priori profile (green), and the $\pm 1\sigma$ uncertainty of the satellite profile (shaded); (middle) the time series of monthly mean ozone partial columns in the 30–40 km and 40-50 km altitude range for the same data sources; and (right) the relative difference between the L3 and retrieved lidar data in this altitude range. This comprehensive comparison illustrates the consistency between satellite and ground-based ozone observations, as well as systematic differences over time and altitude.

https://doi.org/10.5194/egusphere-2025-5728
Preprint. Discussion started: 5 December 2025

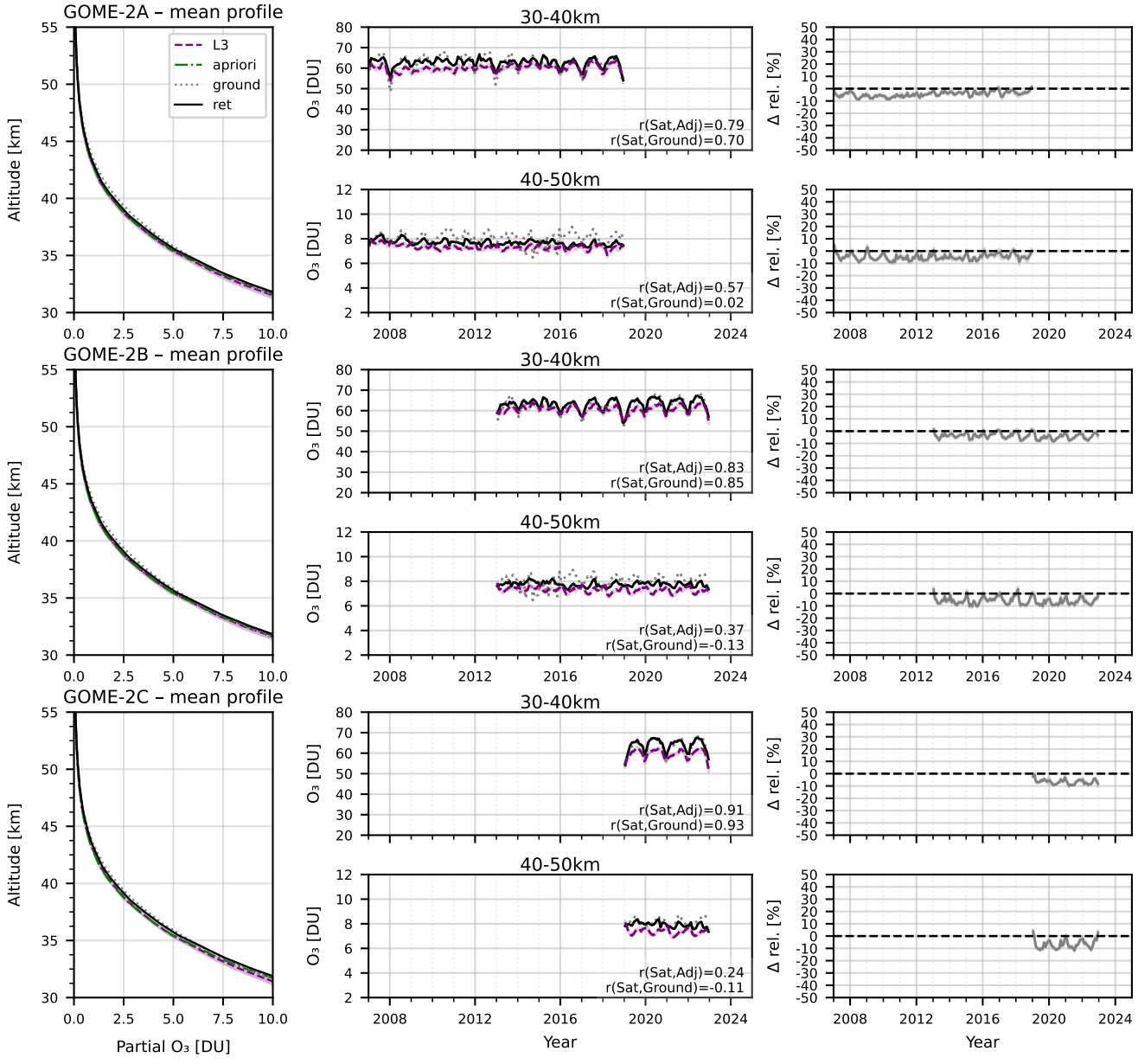

Figure 7. Same as Figure 6 but for all tropical ground-based stations as shown in Figure 4.

https://doi.org/10.5194/egusphere-2025-5728
Preprint. Discussion started: 5 December 2025

Figure 8 illustrates the inter-sensor differences between the three GOME-2 instruments in the upper stratosphere for the altitude ranges 30–40 km (gray line) and 40–50 km (black line), averaged across all mid-latitude stations. The comparison reveals a high degree of consistency among the sensors, with differences generally within 2 DU. The smallest discrepancies are observed in the 40–50 km layer, indicating robust long-term stability in this altitude range.

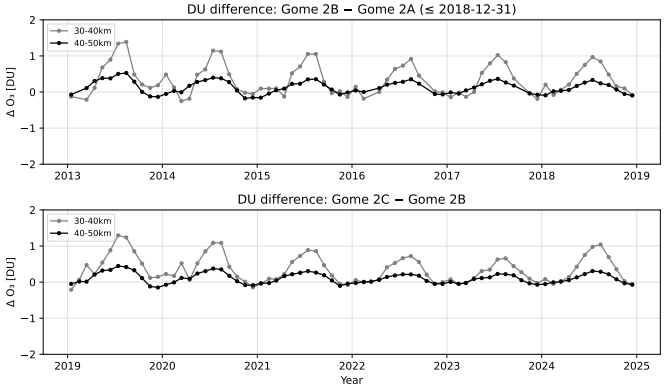

Figure 8. Time series of differences in partial ozone columns (DU) between the GOME-2 satellite pairs for two altitude ranges. **Top:** GOME-2B minus GOME-2A, limited to the period up to 31 December 2018 due to the reduced data quality of GOME-2A. **Bottom:** GOME-2C minus GOME-2B over the respective overlapping time period. Both panels show the altitude ranges 30–40 km (gray line) and 40–50 km (black line).

6 Conclusions

A comparison study of ozone retrieval statistics from the GOME-2 instruments onboard of Metop-A, -B, and -C shows a high level of consistency across latitude bands and atmospheric layers, confirming the maturity and stability of the retrieval algorithm. In the **troposphere**, all three sensors tend to slightly overestimate ozone, with absolute differences (AD) of roughly +1 to +3 DU in mid-latitudes and up to +7.5 DU in the tropics for Metop-C. Relative differences increase toward lower latitudes, reflecting higher retrieval uncertainty under variable cloud and humidity conditions. The standard deviations (STDEV) of 8–15 DU across all sensors indicate robust internal consistency.

In the **lower stratosphere**, all sensors show a small negative bias, typically between -3 and -7 DU (RD ≈ -3 % to -7 %), corresponding to a modest underestimation of ozone concentrations. The lowest scatter is observed for Metop-B (STDEV ≈ 2–3 DU), suggesting particularly stable performance. Regional patterns are coherent across sensors, with slightly weaker negative biases in the tropics and southern mid-latitudes compared to the northern hemisphere.

In the **upper stratosphere**, biases are minimal across all sensors, with absolute difference values, close to zero (-0.1 to -0.4 DU) and extremely low variability (STDEV ≈ 0.1–0.2 DU). These results confirm excellent consistency in the upper-stratospheric ozone retrievals, where radiometric calibration and spectral fitting are least affected by tropospheric interference.

https://doi.org/10.5194/egusphere-2025-5728
Preprint. Discussion started: 5 December 2025

Overall, the three Metop GOME-2 instruments provide mutually consistent ozone profiles with small and systematic inter-satellite differences. The main distinctions are a stronger positive tropospheric bias in Metop-C—particularly in the tropics—and slightly smaller negative deviations in the lower stratosphere for Metop-B. These findings underscore the reliability of the GOME-2 constellation for long-term ozone-trend analyses and the potential for merged multi-sensor time series without significant inter-calibration artifacts.

The observed inter-sensor consistency across Metop-A, -B, and -C supports the creation of a coherent, multi-decadal ozone climate data record. Minor biases in the troposphere and lower stratosphere are small relative to natural ozone variability and can be corrected through standard inter-calibration procedures, ensuring that combined datasets remain robust for trend detection and model evaluation. The minimal deviations in the upper stratosphere further reinforce the stability of GOME-2 instruments over time, making the Metop constellation a reliable backbone for long-term monitoring of ozone distribution, stratosphere-troposphere interactions, and assessment of policy-driven ozone recovery. In conclusion, these results confirm the use of merged Metop GOME-2 datasets in constructing consistent, high-quality ozone time series, suitable for climate and atmospheric research.

Data availability. The level-3 gridded ozone profile data record used for this study can be obtained via the AC SAF helpdesk or via links on the AC SAF website (https://www.acsaf.org/), or via the EUMETSAT Data Center (EUMDC) (https://user.eumetsat.int/data-access/data-centre). Its reserved DOI is: 10.15770/EUM_SAF_AC_0052

Author contributions. OT developed the algorithm, produced the level-2 and gridded the level-3 data. AD and PTA did the analyses of the gridded data and compared them with balloon sondes and LIDAR & microwave respectively. All authors contributed to the interpretation of the results.

Competing interests. There are no competing interests.

Acknowledgements. The authors would like to thank the AC SAF / EUMETSAT for funding the study via the CDOP-4 project, and their ongoing support though GOME-2 L1b data provision. Author AD has received additional funding from PRODEX, contract number 4000140643 B-ACSAF. The data used in this publication were obtained from the Network for the Detection of Atmospheric Composition Change (NDACC) and are available through the NDACC website (NDACC, https://www.ndacc.org). We thank the station Principal Investigators for providing and maintaining the long-term ozonesonde records used in this study.

https://doi.org/10.5194/egusphere-2025-5728
Preprint. Discussion started: 5 December 2025

References

Arosio, C., Sofieva, V., Orfanoz-Cheuquelaf, A., Rozanov, A., Heue, K.-P., Loyola, D., Malina, E., Stauffer, R. M., Tarasick, D., Van Malderen, R., Ziemke, J. R., & Weber, M. (2025). *Intercomparison of tropospheric ozone column datasets from combined nadir and limb satellite observations*. *Atmospheric Measurement Techniques*, 18, 3247–3265. doi:10.5194/amt-18-3247-2025

Bognar, K., Tegtmeier, S., Bourassa, A., Roth, C., Warnock, T., Zawada, D. and Degenstein, D. (2022). Stratospheric ozone trends for 1984–2021 in the SAGE II–OSIRIS–SAGE III/ISS composite dataset. Atmospheric Chemistry and Physics, 22(14), 9553-9569.

Boyd, I. S., A. D. Parrish, L. Froidevaux, T. von Clarmann, E. Kyrölä, J. M. Russell III, and J. M. Zawodny (2007), Ground-based microwave ozone radiometer measurements compared with Aura-MLS v2.2 and other instruments at two Network for Detection of Atmospheric Composition Change sites, J. Geophys. Res., 112, D24S33, doi:10.1029/2007JD008720.

Coldewey-Egbers, M., Loyola-R., D. G., Latter, B., Siddans, R., Kerridge, B., Hubert, D., van Roozendael, M., & Eisinger, M. (2025). *The novel GOME-type Ozone Profile Essential Climate Variable (GOP-ECV) data record covering the past 26 years*. *Atmospheric Measurement Techniques*, 18, 5485–5505. doi:10.5194/amt-18-5485-2025

Delcloo A. (2020): AC SAF Validation report on GOME-2C near real-time and offline global tropospheric ozone https://acsaf.org/docs/vr/Validation_Report_TrO3-C_Jun_2020.pdf

Delcloo A. (2024): AC SAF Validation report on GOME-2 reprocessed global tropospheric ozone. https://acsaf.org/docs/vr/Validation_Report_TrO3_DR_Jan_2024.pdf

Delcloo A., K., Garane, P., Achtert (2020), AC SAF Validation report on GOME-2 near real-time ozone profiles for GOME-2C. https://acsaf.org/docs/vr/Validation_Report_NHP-C_OHP-C_Jun_2020.pdf.

Delcloo A., K., Garane, P., Achtert (2024), AC SAF Validation report on GOME-2 near real-time and reprocessed ozone profiles. https://acsaf.org/docs/vr/Validation_Report_O3_prof_DR_Jan_2024.pdf

EUMETSAT (2022), GOME-2 Metop-A and -B FDR Product Validation Report Reprocessing R3, (EUM/OPS/DOC/21/1237264), EUMETSAT, 4e, 2022, https://user.eumetsat.int/

Gaudel, A., Bourgeois, I., Li, M., Chang, K.-L., Ziemke, J., Sauvage, B., Stauffer, R. M., Thompson, A. M., Kollonige, D. E., Smith, N., Hubert, D., Keppens, A., Cuesta, J., Heue, K.-P., Veefkind, P., Aikin, K., Peischl, J., Thompson, C. R., Ryerson, T. B., Frost, G. J., McDonald, B. C., & Cooper, O. R. (2024). *Tropical tropospheric ozone distribution and trends from in situ and satellite data*. *Atmospheric Chemistry and Physics*, 24, 9975–10000. doi:10.5194/acp-24-9975-2024

Godin S., G. Megie, J. Pelon: Systematic lidar measurements of the stratospheric ozone vertical distribution, GRL, 16, 6, doi/10.1029/GL016i006p00547, 1998

Godin-Beekmann, S., Azouz, N., Sofieva, V. F., Hubert, D., Petropavlovskikh, I., Effertz, P., Ancellet, G., Degenstein, D. A., Zawada, D., Froidevaux, L., Frith, S., Wild, J., Davis, S., Steinbrecht, W., Leblanc, T., Querel, R., Tourpali, K., Damadeo, R., Maillard Barras, E., Stübi, R., Vigouroux, C., Arosio, C., Nedoluha, G., Boyd, I., Van Malderen, R., Mahieu, E., Smale, D., and Sussmann, R.: Updated trends of the stratospheric ozone vertical distribution in the 60° S–60° N latitude range based on the LOTUS regression model , Atmos. Chem. Phys., 22, 11657–11673, https://doi.org/10.5194/acp-22-11657-2022, 2022.

García, O. E., Sanromá, E., Schneider, M., Hase, F., León-Luis, S. F., Blumenstock, T., Sepúlveda, E., Redondas, A., Carreño, V., Torres, C., and Prats, N.: Improved ozone monitoring by ground-based FTIR spectrometry, Atmos. Meas. Tech., 15, 2557–2577, https://doi.org/10.5194/amt-15-2557-2022, 2022

https://doi.org/10.5194/egusphere-2025-5728
Preprint. Discussion started: 5 December 2025

Hocke, K., Kämpfer, N., Ruffieux, D., Froidevaux, L., Parrish, A., Boyd, I., von Clarmann, T., Steck, T., Timofeyev, Y. M., Polyakov, A. V., and Kyrölä, E.: Comparison and synergy of stratospheric ozone measurements by satellite limb sounders and the ground-based microwave radiometer SOMORA, Atmos. Chem. Phys., 7, 4117–4131, https://doi.org/10.5194/acp-7-4117-2007, 2007.

Johnson, M. S., Liu, X., Zoogman, P., Sullivan, J., Newchurch, M. J., Kuang, S., Leblanc, T. and McGee, T., Evaluation of potential sources of a priori ozone profiles for TEMPO tropospheric ozone retrievals, Atmospheric Measurement Techniques, 11, 6, 3457–3477, https://amt.copernicus.org/articles/11/3457/2018/, 10.5194/amt-11-3457-2018, 2018

Keckhut, Philippe, et al. "Review of ozone and temperature lidar validations performed within the framework of the Network for the Detection of Stratospheric Change." Journal of Environmental Monitoring 6.9 (2004): 721-733, https://doi.org/10.1029/GL016i006p00547.

Keppens, A., Hubert, D., Granville, J., Nath, O., Lambert, J.-C., Wespes, C., Coheur, P.-F., Clerbaux, C., Boynard, A., Siddans, R., Latter, B., Kerridge, B., Di Pede, S., Veefkind, P., Cuesta, J., Dufour, G., Heue, K.-P., Coldewey-Egbers, M., Loyola, D., Orfanoz-Cheuquelaf, A., Maratt Satheesan, S., Eichmann, K.-U., Rozanov, A., Sofieva, V. F., Ziemke, J. R., Inness, A., Van Malderen, R., & Hoffmann, L. (2025). *Harmonisation of sixteen tropospheric ozone satellite data records*. *EGUsphere* [preprint]. doi:10.5194/egusphere-2024-3746

Leblanc, T., and I. S. McDermid, Stratospheric Ozone Climatology From Lidar Measurements at Table Mountain (34.4°N, 117.7°W) and Mauna Loa (19.5°N, 155.6°W), J. Geophysical Research, 105, 14,613-14,623, 2000.

Lobsiger E., K.F. Künzi and H.U. Dütsch, Comparison of stratospheric ozone profiles retreived from microwave-radiometer and Dobson-spectrometer data, J. Atm. and Terr. Phys., 46, 799-806, 1984.

McPeters, R. D. and Labow, G. J., Climatology 2011: An MLS and sonde derived ozone climatology for satellite retrieval algorithms, Journal of Geophysical Research (Atmospheres), 117, D10, 2156–2202, doi:10.1029/2011JD017006".

Okamoto, S., Cuesta, J., Dufour, G., Eremenko, M., Miyazaki, K., Boonne, C., Tanimoto, H., Peischl, J. and Thompson, C. (2024). *Natural and anthropogenic influence on tropospheric ozone variability over the Tropical Atlantic unveiled by satellite and in situ observations*. *EGUsphere* [preprint]. doi:10.5194/egusphere-2024-3758

Parrish, A., R.L. de Zafra, P.M. Solomon, and J.W. Barrett, A ground-based technique for millimeter wave spectroscopic observations of stratospheric trace constituents, Radio Sci., 23, 106-118, 1988.

Rodgers C.D., Characterization and Error Analysis of Profiles Retrieved from Remote Sounding Measurements, J. Geophys. Res., 95, 5587-5595, 1990.

Smit, H. G. J., Straeter, W., Johnson, B. J., Oltmans, S. J., Davies, J., Tarasick, D. W., Hoegger, B., Stübi, R., Schmidlin, F. J., Northam, T., Thompson, A. M., Witte, J. C., Boyd, I., Posny, F. (2007). Assessment of the performance of ECC-ozonesondes under quasi-flight conditions in the environmental simulation chamber: Insights from the Jülich Ozone Sonde Intercomparison Experiment (JOSIE). *Journal of Geophysical Research*, 112, D19306. doi:10.1029/2006JD007308.

Spurr, R., de Haan, J., and van Oss, R., and Vasilkov, A., Discrete-ordinate radiative transfer in a stratified medium with first-order rotational Raman scattering, Journal of Quantitative Spectroscopy & Radiative Transfer, 2008, 109, 404-425, doi:10.1016/j.jqsrt.2007.08.011.

Stauffer, R. M., Thompson, A. M., Kollonige, D. E., Tarasick, D. W., Van Malderen, R., Smit, H. G. J., et al. (2022). An examination of the recent stability of ozonesonde global network data. Earth and Space Science, 9, e2022EA002459. https://doi.org/10.1029/2022EA002459

Steinbrecht W., et al. (2006), Long-term evolution of upper stratospheric ozone at selected stations of the Network for the Detection of Stratospheric Change (NDSC), J. Geophys. Res., 111, D10308, doi:10.1029/2005J

Steinbrecht, W., Froidevaux, L., Fuller, R., Wang, R., Anderson, J., Roth, C., Bourassa, A., Degenstein, D., Damadeo, R., Zawodny, J., Frith, S., McPeters, R., Bhartia, P., Wild, J., Long, C., Davis, S., Rosenlof, K., Sofieva, V., Walker, K., Rahpoe, N., Rozanov, A., Weber,

https://doi.org/10.5194/egusphere-2025-5728
Preprint. Discussion started: 5 December 2025

M., Laeng, A., von Clarmann, T., Stiller, G., Kramarova, N., Godin-Beekmann, S., Leblanc, T., Querel, R., Swart, D., Boyd, I., Hocke, K., Kämpfer, N., Maillard Barras, E., Moreira, L., Nedoluha, G., Vigouroux, C., Blumenstock, T., Schneider, M., García, O., Jones, N., Mahieu, E., Smale, D., Kotkamp, M., Robinson, J., Petropavlovskikh, I., Harris, N., Hassler, B., Hubert, D., and Tummon, F.: An update on ozone profile trends for the period 2000 to 2016, Atmos. Chem. Phys., 17, 10675–10690, https://doi.org/10.5194/acp-17-10675-2017, 2017.

Steinbrecht, W., Velazco, V. A., Dirksen, R., Doppler, L., Oelsner, P., Van Malderen, R., et al. (2025). Ground-based monitoring of stratospheric ozone and temperature over Germany since the 1960s. Earth and Space Science, 12, e2024EA003821. https://doi.org/10.1029/2024EA003821

L.G. Tilstra, O.N.E. Tuinder, P. Wang, and P. Stammes, Surface reflectivity climatologies from UV to NIR determined from Earth observations by GOME-2 and SCIAMACHY, J. Geophys. Res. Atmos. 122, 4084-4111, doi:10.1002/2016JD025940, 2017.

L.G. Tilstra, O.N.E. Tuinder, P. Wang, and P. Stammes, Directionally dependent Lambertian-equivalent reflectivity (DLER) of the Earth's surface measured by the GOME-2 satellite instruments, Atmos. Meas. Tech. 14, 4219-4238, doi:10.5194/amt-14-4219-2021, 2021.

Tuinder, O. N. E., and van Oss, R. F., de Haan, J., and Delcloo, A., ACSAF Algorithm Theoretical Basis Document for NRT and Offline Vertical Ozone Profile and Tropospheric Ozone Column Products, ATBD, 2.1.3, 2022; https://acsaf.org/atbds.php.

Smit, H. G. J., Poyraz, D., Van Malderen, R., Thompson, A. M., Tarasick, D. W., Stauffer, R. M., Johnson, B. J., and Kollonige, D. E.: New insights from the Jülich Ozone Sonde Intercomparison Experiment: calibration functions traceable to one ozone reference instrument, *Atmospheric Measurement Techniques*, **17**, 73–112, 2024, https://amt.copernicus.org/articles/17/73/2024/, doi: 10.5194/amt-17-73-2024.

Stübi, R., Levrat, G., Hoegger, B., Viatte, P., Staehelin, J., Schmidlin, F. J. (2008). In-flight comparison of Brewer–Mast and electrochemical concentration cell ozonesondes. *Journal of Geophysical Research*, 113, D13302. doi:10.1029/2007JD009091.

Smit, H. G. J. and the ASOPOS Panel (2014). *Quality assurance and quality control for ozonesonde measurements in GAW*. WMO/-GAW Report No. 201. Geneva: World Meteorological Organization. Available at: https://www.en-sci.com/wp-content/uploads/2018/05/GAW-Report-201-Quality-Assurance-and-Quality-Control-For-Ozonesonde-Measurements-In-GAW.pdf

WMO: Scientific assessment of ozone depletion: 2018. Global Ozone Research and Monitoring Project Report no. 58, Geneva, Switzerland: World Meteorological Organization, ISBN: 978-1-7329317-1-8, 2018.

WMO: Scientific assessment of ozone depletion: Global Ozone Research and Monitoring Project – GAW Report no. 278, Geneva, Switzerland: World Meteorological Organization, ISBN: 978-9914-733-97-6, 2022.